

## Effect of Longitudinal Roughness on Magnetic Fluid Based Squeeze Film between Truncated Conical Plates

P.I. Andharia<sup>1</sup> and G.M. Deheri<sup>2</sup>

**Abstract:** An attempt has been made to study and analyze the performance of a magnetic fluid based squeeze film between rough truncated conical plates. The lubricant used here is a magnetic fluid and the external magnetic field is oblique to the lower plate. The bearing surfaces are assumed to be longitudinally rough. The roughness of the bearing surfaces is modeled by a stochastic random variable with nonzero mean, variance and skewness. Efforts have been made to average the associated Reynolds equation with respect to the random roughness parameter. The concerned non-dimensional equation is solved with appropriate boundary conditions in dimensionless form to obtain the pressure distribution. This is then used to get the expression for load carrying capacity, resulting in the calculation of response time. The results are presented graphically. It is observed that the bearing system registers an improved performance as compared to that of a bearing system dealing with a conventional lubricant. The results indicate that the pressure, load carrying capacity and response time increase with increasing magnetization parameter. This investigation reveals that the standard deviation induces a positive effect (unlike the case of transverse roughness). Besides, negatively skewed roughness increases the load carrying capacity and this performance further enhances especially when negative variance is involved. Although, aspect ratio and semi-vertical angle tend to decrease the load carrying capacity, there is a scope for obtaining better performance in the case of negatively skewed roughness.

**Keywords:** Magnetic fluid, longitudinal roughness, squeeze film, truncated conical plates, load carrying capacity, Reynolds equation.

### Nomenclature

$a, b$  dimensions of the bearing  
 $h_0$  central film thickness

---

<sup>1</sup> Department of Mathematics, Bhavnagar University, Bhavnagar, Gujarat, India.

<sup>2</sup> Department of Mathematics, S.P. University, Vallabh Vidyanagar, Gujarat, India.

$h_1$	initial film thickness
$h_2$	film thickness after time $\Delta t$
$\bar{h}_1$	$h_1/h_0$
$\bar{h}_2$	$h_2/h_0$
$k$	aspect ratio $b/a$
$\bar{M}$	magnetic field
$M^2$	magnitude of magnetic field
$p$	pressure in the film region
$\bar{p}$	expected value of the pressure
$P$	non-dimensional film pressure
$t$	time
$w$	load capacity
$W$	non-dimensional load capacity
$x, y, z$	Cartesian co-ordinates (' $x$ ' measuring distance along the film in the plane of the figure)
$\alpha$	mean of the stochastic film thickness
$\sigma$	standard deviation of the stochastic film thickness
$\varepsilon$	measure of symmetry of the stochastic film thickness
$\sigma^2$	variance
$\omega$	semi-vertical angle of the cone
$\mu$	fluid viscosity
$\bar{\mu}$	magnetic susceptibility
$\mu^*$	dimensionless magnetization parameter
$\mu_0$	permeability of the free space
$\Delta t$	time required for the film thickness to decrease to a value $h_2$
$\Delta T$	non-dimensional squeeze time

## 1 Introduction

The transient load carrying capacity of a fluid film between two surfaces having a relative normal velocity plays an important role in frictional devices such as clutch plates in automobile transmissions. The behaviour of a squeeze film between various geometrical configurations was analyzed by Archibald (1956). Subsequently, Wu (1970, 1972) discussed the squeeze film performance for mainly, two types of geometry namely, annular and rectangular when one of the surfaces was porous faced. Prakash and Vij (1973) investigated the load capacity and time height relation for squeeze film between porous plates. In this paper they considered various geometries like circular, annular, elliptical, rectangular, conical and truncated conical. A comparison was made between the squeeze film performance of various

geometries of equivalent surface area and it was proved that the circular geometry admitted the highest transient load carrying capacity, other parameters remaining same. Murti (1975) studied the behaviour of the squeeze film entrapped between curved circular plates describing the film thickness by an exponential expression. This analysis of Murti was further modified and developed by Gupta and Vora (1980) to discuss the squeeze film performance between curved annular plates.

All the above studies considered conventional lubricant. The application of a magnetic fluid as a lubricant was investigated by Verma (1986). The magnetic fluid consisted of fine magnetic grains coated with a surfactant and dispersed in a non conducting magnetically passive solvent. Subsequently the squeeze film between porous annular disks was analyzed by Bhat and Deheri (1991) taking a magnetic fluid lubricant with the external magnetic field oblique to the lower disk. This analysis was improved further by Bhat and Deheri (1992) to deal with the performance of a magnetic fluid based squeeze film between curved circular plates. Patel and Deheri (2002a, 2002b) analyzed magnetic fluid based squeeze film between two curved plates lying along the surfaces determined by secant and hyperbolic functions. Furthermore, Patel and Deheri (2007) dealt with the behaviour of a magnetic fluid based squeeze film between porous conical plates.

It is a well known fact that the bearing surfaces after having some run-in and wear develop roughness. Besides, due to elastic thermal and uneven wear effects the configuration encountered in practice are usually far from smooth. The effect of surface roughness was studied and analyzed by many investigators [Davies (1963), Burton (1963), Michell (1950), Tonder (1972) and Tzeng and Saibel (1967)]. Christensen and Tonder (1969a, 1969b, 1970) mathematically modeled the random roughness and suggested a comprehensive general analysis for investigating the effect of transverse as well as longitudinal surface roughness. This approach of Christensen and Tonder (1969a, 1969b, 1970) was the foundation for analyzing the effect of surface roughness in a number of investigations [Ting (1975), Prakash and Tiwari (1982, 1983), Prajapati (1991, 1992), Guha (1993), Gupta and Deheri (1996) and Andharia, Gupta and Deheri (1997)]. Deheri, Andharia and Patel (2004) studied the effect of longitudinal roughness on the performance of slider bearings with squeeze film formed by a magnetic fluid. Recently Andharia and Deheri (2010) discussed the longitudinal roughness effect on the performance of a squeeze film in conical plates under the presence of a magnetic fluid lubricant. These above two studies established that the standard deviation associated with the longitudinal surface roughness increases the load carrying capacity.

Therefore, it has been proposed to study the effect of longitudinal surface roughness on the behaviour of magnetic fluid based squeeze film between truncated conical plates.

## 2 Analysis

The configuration of the bearing is shown in Fig. 1. Squeeze film velocity  $\frac{dh_0}{dt}$  in the Z-direction. The magnetic field  $\bar{M}$  is oblique to the lower plate.

The assumptions of usual hydrodynamic lubrication theory are taken into consideration in the analysis. The lubricant film is considered to be isoviscous and incompressible and the flow is laminar.

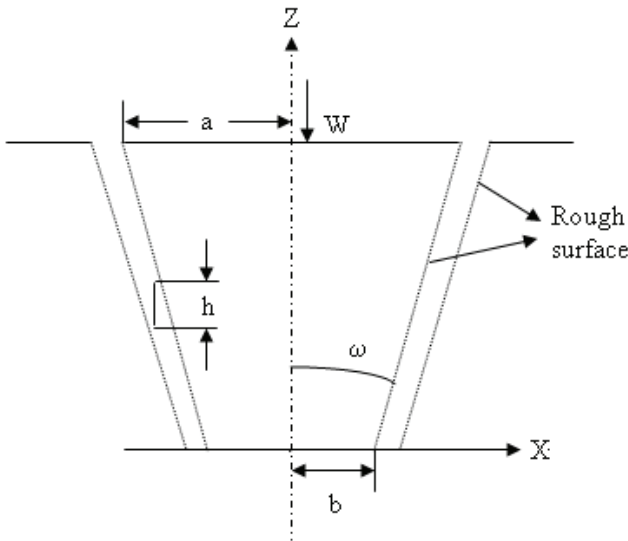


Figure 1: Configuration of the problem

The bearing surfaces are assumed to be longitudinally rough. Following Christensen and Tonder (1969a, 1969b, 1970), the thickness  $h$  of the lubricant film is

$$h = \bar{h} + h_s \quad (1)$$

where  $\bar{h}$  is the mean film thickness and  $h_s$  is the deviation from the mean film thickness characterizing the random roughness of the bearing surfaces.  $h_s$  is considered to be stochastic in nature and governed by the probability density function  $f(h_s)$ ,  $-c \leq h_s \leq c$ , where  $c$  is the maximum deviation from the mean film thickness. The mean  $\bar{\alpha}$ , the standard deviation  $\bar{\sigma}$  and the parameter  $\bar{\epsilon}$  which is the measure of symmetry, of the random variable  $h_s$ , are defined by the relationships:

$$\bar{\alpha} = E(h_s)$$

$$\bar{\sigma}^2 = E \left[ (h_s - \bar{\alpha})^2 \right]$$

and

$$\bar{\varepsilon} = E \left[ (h_s - \bar{\alpha})^3 \right] \tag{2}$$

where  $E$  denotes the expected value defined by

$$E(R) = \int_{-c}^c Rf(h_s)dh_s \tag{3}$$

wherein [Tzeng and Saibel (1967)]

$$f(h_s) = \begin{cases} \frac{35}{32} \left( 1 - \frac{h_s^2}{c^2} \right)^3, & -c \leq h_s \leq c \\ 0, & \text{otherwise} \end{cases} \tag{4}$$

Axially symmetric flow of magnetic fluid between the truncated conical plates is taken into consideration under an oblique magnetic field  $\bar{M}$  whose magnitude  $M$  is given by [Patel and Deheri (2007)]

$$M^2 = K(a \cos ec \omega - x)(x - b \cos ec \omega), \quad b < x < a, \tag{5}$$

where  $a$  and  $b$  are dimensions of the bearing. Here  $K$  is suitably chosen so as to have a magnetic field of required strength, which suits the bearing dimensions. The direction of the magnetic field is significant since  $\bar{M}$  has to satisfy the equations

$$\nabla \cdot \bar{M} = 0, \quad \nabla \times \bar{M} = 0 \tag{6}$$

Thus,  $\bar{M}$  arises out of a potential function and the inclination angle  $\theta$  of the magnetic field  $\bar{M}$  with the lower plate is determined from [Bhat (2003)]

$$\cot \theta \frac{\partial \theta}{\partial x} + \frac{\partial \theta}{\partial z} = \frac{bx - a \cos ec \omega}{b \cos ec \omega (xa \cos ec \omega - x^2)} \tag{7}$$

whose solution is determined from the equations [Bhat (2003)]

$$\cos ec^2 \theta = C^2 (xa \cos ec \omega - x^2)$$

$$C(2x - b \cos ec \omega) = [C^2 a^2 \cos ec^2 \omega - 4 \sin(Cz)]^{1/2}, \tag{8}$$

C being an arbitrary constant. The modified Reynolds' equation [Prakash and Vij (1973), Patel and Deheri (2007)] governing the film pressure  $p$  in the present case is obtained as

$$\frac{1}{x} \frac{d}{dx} \left[ x h^3 \frac{d}{dx} (p - 0.5 \mu_0 \bar{\mu} M^2) \right] = \frac{12 \mu \dot{h}_0}{\sin^2 \omega} \quad (9)$$

where  $h$  is film thickness,  $\omega$  is semi-vertical angle of cone,  $\mu$  is fluid viscosity,  $\bar{\mu}$  represents the magnetic susceptibility and  $\mu_0$  stands for permeability of the free space.

It is easily observed that  $\bar{\alpha}$ ,  $\bar{\sigma}$  and  $\bar{\varepsilon}$  are all independent of  $x$  and while  $\bar{\alpha}$  and  $\bar{\varepsilon}$  can assume both positive and negative values,  $\bar{\sigma}$  is always positive. Following the average process discussed by Andharia, Gupta and Deheri (1997) and using Eq.5, Eq.9 takes the form

$$\frac{1}{x} \frac{d}{dx} \left[ x m(\bar{h})^{-1} \frac{d}{dx} (\bar{p} - 0.5 \mu_0 \bar{\mu} K (a \operatorname{cosec} \omega - x)(x - b \operatorname{cosec} \omega)) \right] = \frac{12 \mu \dot{h}_0}{\sin^2 \omega} \quad (10)$$

where  $\bar{p}$  is the expected value of the lubricant pressure  $p$  while

$$m(\bar{h}) = \bar{h}^{-3} \left[ 1 - 3 \bar{\alpha} \bar{h}^{-1} + 6 \bar{h}^{-2} (\bar{\sigma}^2 + \bar{\alpha}^2) - 20 \bar{h}^{-3} (\bar{\varepsilon} + 3 \bar{\sigma}^2 \bar{\alpha} + \bar{\alpha}^3) \right] \quad (11)$$

Introducing dimensionless quantities

$$H = \frac{\bar{h}}{h_0}, \quad X = \frac{x}{a}, \quad M(H) = h_0^3 m(\bar{h}), \quad \alpha = \frac{\bar{\alpha}}{h_0}, \quad \sigma = \frac{\bar{\sigma}}{h_0}, \quad \varepsilon = \frac{\bar{\varepsilon}}{h_0^3}, \quad k = \frac{b}{a},$$

$$\mu^* = \frac{-\mu_0 \bar{\mu} h_0^3 k}{\mu \dot{h}_0} \text{ and } P = \frac{-\bar{p} h_0^3}{\mu \dot{h}_0 \pi (a^2 - b^2) \operatorname{cosec} \omega}, \quad (12)$$

Eq.10 becomes

$$\frac{1}{X} \frac{d}{dX} \left[ X M(H)^{-1} \frac{d}{dX} \left( P - \frac{0.5 \mu^* (1 - X \sin \omega)(X - k \operatorname{cosec} \omega)}{\pi (1 - k^2)} \right) \right] = \frac{12 \operatorname{cosec} \omega}{\pi (k^2 - 1)} \quad (13)$$

The associated boundary conditions are

$$P(k \operatorname{cosec} \omega) = 0; \quad P(\operatorname{cosec} \omega) = 0 \quad (14)$$

Integrating Eq.13 and using boundary condition  $P(k \cos ec \omega) = 0$ , we get

$$\frac{d}{dX} \left( P - \frac{0.5\mu^*(1-X \sin \omega)(X - k \cos ec \omega)}{\pi(1-k^2)} \right) = \frac{6M(H)k^2 \cos ec^3 \omega}{\pi(1-k^2)} \frac{1}{X} - \frac{6M(H) \cos ec \omega}{\pi(1-k^2)} X \quad (15)$$

Integrating Eq.15 with the use of boundary condition  $P = 0$  at  $X = \cos ec \omega$ , the dimensionless pressure is obtained as

$$P = \frac{1}{2\pi(1-k^2)} \left[ \mu^*(1-X \sin \omega)(X - k \cos ec \omega) + 6M(H) \cos ec^3 \omega \left\{ (1-X^2 \sin^2 \omega) + 2k^2 \ln(X \sin \omega) \right\} \right] \quad (16)$$

where

$$M(H) = H^{-3} \left[ 1 - 3\alpha H^{-1} + 6H^{-2} (\sigma^2 + \alpha^2) - 20H^{-3} (\epsilon + 3\sigma^2 \alpha + \alpha^3) \right] \quad (17)$$

The load carrying capacity

$$w = 2\pi \int_{b \cos ec \omega}^{a \cos ec \omega} x p dx \quad (18)$$

of the bearing in non-dimensional form can be expressed as

$$\begin{aligned} W &= \frac{-wh_0^3}{\mu \dot{h}_0 (a^2 - b^2)^2 \pi^2 \cos ec^2 \omega} \\ &= \frac{2}{(1-k^2) \cos ec \omega} \int_{k \cos ec \omega}^{\cos ec \omega} X P dX \\ &= \frac{\mu^*(1-k)^2 \cos ec^3 \omega}{24\pi} + \frac{3M(H) \cos ec^5 \omega}{4\pi(1-k^2)} [(1-k^2)(1-3k^2) - 4k^4 \ln(k)] \end{aligned} \quad (19)$$

If the time taken by the plate to move from the film thickness  $h_1$  (at time  $t_1$ ) to  $h_2$  (at time  $t_2$ ), then the dimensionless squeeze time  $\Delta T$  is obtained from Eq.19 as

$$\begin{aligned} \Delta T &= \frac{wh_0^2}{\mu \pi^2 (a^2 - b^2) \cos ec^2 \omega} \Delta t \\ &= \frac{W}{2} \left( \frac{1}{h_2^2} - \frac{1}{h_1^2} \right) \end{aligned} \quad (20)$$

where

$$\bar{h}_1 = \frac{h_1}{h_0} \text{ and } \bar{h}_2 = \frac{h_2}{h_0}. \quad (21)$$

### 3 Results and Discussion

It is clearly seen from Eqs. 16, 19 and 20 that the dimensionless pressure, load carrying capacity and response time depend on various parameters such as  $\mu^*$ ,  $\sigma$ ,  $\alpha$ ,  $\varepsilon$ ,  $\omega$  and  $k$ . These parameters described respectively, the effect of magnetic fluid lubricant, longitudinal roughness, angle associated with the truncated cone and the aspect ratio. Further, Eq.16 and Eq.19 suggest that the pressure increases by

$$\frac{\mu^*(1 - X \sin \omega)(X - k \operatorname{cosec} \omega)}{2\pi(1 - k^2)} \quad (22)$$

while the load carrying capacity enhances by

$$\frac{\mu^*(1 - k)^2 \operatorname{cosec}^3 \omega}{24\pi} \quad (23)$$

It is clear that setting the roughness parameters to be zero one obtains the discussions carried out by Patel and Deheri (2007) in the absence of porosity. Further, taking  $\mu^*$  as zero this investigation reduces to the study of Prakash and Vij (1973) concerning the truncated conical plates in the absence of porosity. Also, Eqs. 16, 19 and 20 suggest that the pressure, load carrying capacity and response time increase with the magnetization parameter.

Figs. 2 – 9 present the distribution of load carrying capacity with respect to the magnetization parameter  $\mu^*$  for various values of roughness parameters, semi-vertical angle and aspect ratio. These figures show that the load carrying capacity increases marginally with respect to the magnetization parameter  $\mu^*$  while it decreases substantially due to semi-vertical angle and the aspect ratio. Figs. 2 – 4 makes it clear that the load carrying capacity decreases due to  $\alpha$  (+ve) and  $\varepsilon$  (+ve). However, standard deviation ( $\sigma$ ) increases the load carrying capacity. Further, negatively skewed roughness improves the performance of the bearing system and so is the case with negative variance. In addition, it is revealed that the effect of the semi-vertical angle is relatively sharp as compared to that of aspect ratio. Of course, the combined effect of negative variance, negatively skewed roughness and the standard deviation presents a considerably better performance, while the combined effect of  $\alpha$  (+ve) and  $\varepsilon$  (+ve) leads to a reduced load carrying capacity. In Figs. 10 – 13 one can have the variation of load carrying capacity with respect

to the semi-vertical angle for various values of variance, skewness, standard deviation and the aspect ratio. A close look at these figures indicates that the aspect ratio plays a prominent role in reducing the load carrying capacity. The effect of standard deviation turns out to be positive which is indicated by Figs. 4 and 7. Figs. 14 – 17 present the profile of the load carrying capacity with respect to the aspect ratio for various values of variance, skewness, standard deviation and the semi-vertical angle. From these figures it is clearly seen that the aspect ratio may play a crucial role in designing the bearing system. The combined effect of the aspect ratio and the standard deviation is really appealing in the case of negatively skewed roughness in presence of negative variance.

Lastly, it is clear from Eq.20 that the response time almost follows the trends of load carrying capacity.

This investigation offers the suggestion that the effect of negatively skewed roughness is slightly better than the effect of negative variance with respect to the semi-

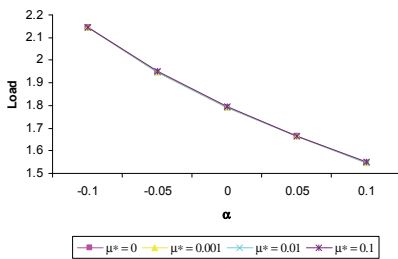


Figure 2: Variation of load carrying capacity with respect to  $\alpha$  and  $\mu^*$  for  $k = 0.5$ ,  $\omega = 50^\circ$ ,  $\epsilon = -0.05$  and  $\sigma = 0.05$ .

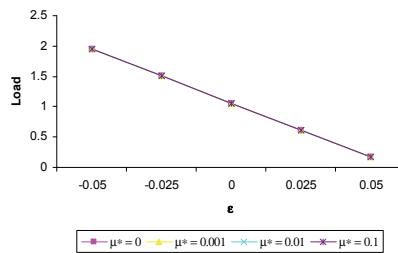


Figure 3: Variation of load carrying capacity with respect to  $\epsilon$  and  $\mu^*$  for  $k = 0.5$ ,  $\omega = 50^\circ$ ,  $\alpha = -0.05$  and  $\sigma = 0.05$ .

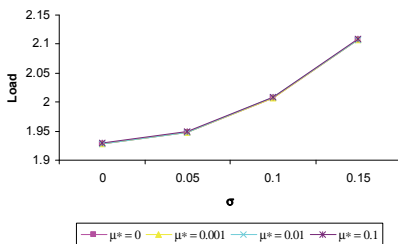


Figure 4: Variation of load carrying capacity with respect to  $\sigma$  and  $\mu^*$  for  $k = 0.5$ ,  $\omega = 50^\circ$ ,  $\alpha = -0.05$  and  $\epsilon = -0.05$ .

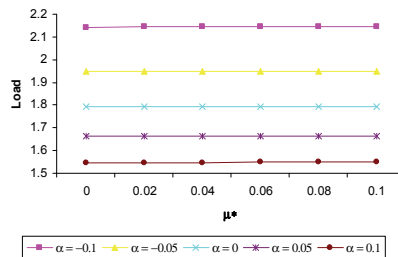


Figure 5: Variation of load carrying capacity with respect to  $\mu^*$  and  $\alpha$  for  $k = 0.5$ ,  $\omega = 50^\circ$ ,  $\epsilon = -0.05$  and  $\sigma = 0.05$ .

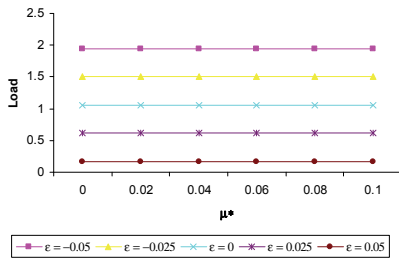


Figure 6: Variation of load carrying capacity with respect to  $\mu^*$  and  $\epsilon$  for  $k = 0.5$ ,  $\omega = 50^\circ$ ,  $\alpha = -0.05$  and  $\sigma = 0.05$ .

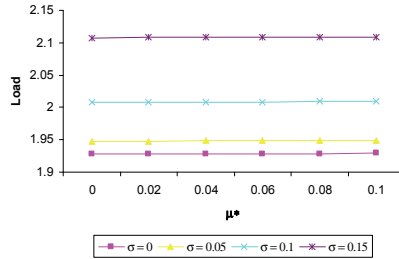


Figure 7: Variation of load carrying capacity with respect to  $\mu^*$  and  $\sigma$  for  $k = 0.5$ ,  $\omega = 50^\circ$ ,  $\alpha = -0.05$  and  $\epsilon = -0.05$ .

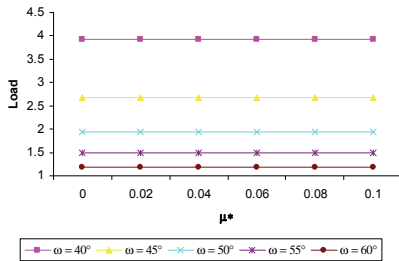


Figure 8: Variation of load carrying capacity with respect to  $\mu^*$  and  $\omega$  for  $k = 0.5$ ,  $\alpha = -0.05$ ,  $\epsilon = -0.05$  and  $\sigma = 0.05$ .

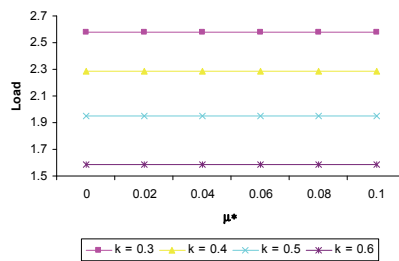


Figure 9: Variation of load carrying capacity with respect to  $\mu^*$  and  $k$  for  $\omega = 50^\circ$ ,  $\alpha = -0.05$ ,  $\epsilon = -0.05$  and  $\sigma = 0.05$ .

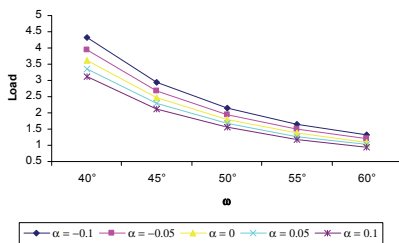


Figure 10: Variation of load carrying capacity with respect to  $\omega$  and  $\alpha$  for  $k = 0.5$ ,  $\mu^* = 0.01$ ,  $\epsilon = -0.05$  and  $\sigma = 0.05$ .

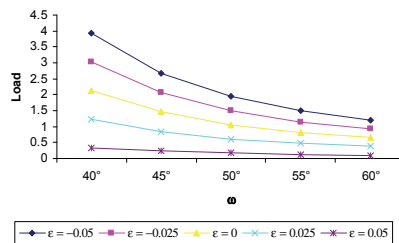


Figure 11: Variation of load carrying capacity with respect to  $\omega$  and  $\epsilon$  for  $k = 0.5$ ,  $\mu^* = 0.01$ ,  $\alpha = -0.05$  and  $\sigma = 0.05$ .

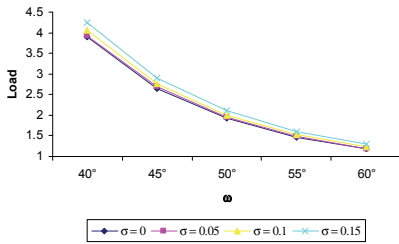


Figure 12: Variation of load carrying capacity with respect to  $\omega$  and  $\sigma$  for  $k = 0.5$ ,  $\mu^* = 0.01$ ,  $\alpha = -0.05$  and  $\varepsilon = -0.05$ .

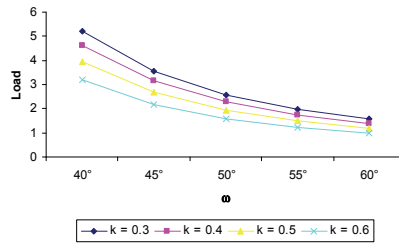


Figure 13: Variation of load carrying capacity with respect to  $\omega$  and  $k$  for  $\mu^* = 0.01$ ,  $\alpha = -0.05$ ,  $\varepsilon = -0.05$  and  $\sigma = 0.05$ .

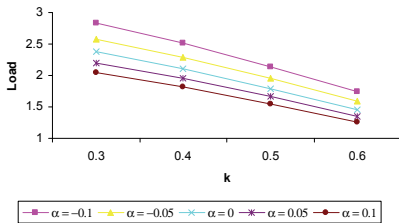


Figure 14: Variation of load carrying capacity with respect to  $k$  and  $\alpha$  for  $\omega = 50^\circ$ ,  $\mu^* = 0.01$ ,  $\varepsilon = -0.05$  and  $\sigma = 0.05$ .

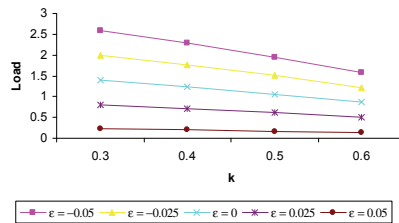


Figure 15: Variation of load carrying capacity with respect to  $k$  and  $\varepsilon$  for  $\omega = 50^\circ$ ,  $\mu^* = 0.01$ ,  $\alpha = -0.05$  and  $\sigma = 0.05$ .

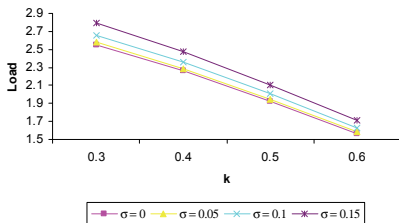


Figure 16: Variation of load carrying capacity with respect to  $k$  and  $\sigma$  for  $\omega = 50^\circ$ ,  $\mu^* = 0.01$ ,  $\alpha = -0.05$  and  $\varepsilon = -0.05$ .

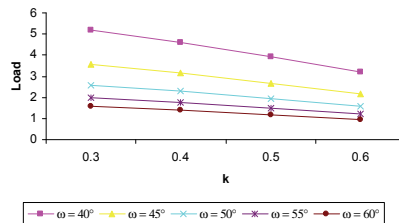


Figure 17: Variation of load carrying capacity with respect to  $k$  and  $\omega$  for  $\mu^* = 0.01$ ,  $\alpha = -0.05$ ,  $\varepsilon = -0.05$  and  $\sigma = 0.05$ .

vertical angle and the aspect ratio. However, the effect of standard deviation with respect to the semi vertical angle is a little better than its effect with respect to the aspect ratio. It is interesting to observe that the combined effect of magnetization parameter and standard deviation prevents the response time to fall rapidly for suitable choices of aspect ratio and semi vertical angle.

#### 4 Conclusion

This article tends to suggest that the negative effect induced by positive variance, semi-vertical angle and the aspect ratio can be considerably reduced by the positive effect of magnetization parameter and standard deviation in the case of negatively skewed roughness. Thus, this investigation establishes that there exist sufficient scopes for enhancing the performance of a longitudinally rough bearing system by suitably choosing magnetization parameter, radii ratio and semi-vertical angle of the cone. The importance of this study lies in the fact that besides providing additional degree of freedom it offers ample scopes for having improved performances. In addition this investigation makes it mandatory to account for roughness while designing such magnetic fluid based bearing system even if a proper choice of angle – aspect ratio combination has been considered especially, from life period point of view.

**Acknowledgement:** The authors gratefully acknowledge the critical comments and fruitful suggestions of the reviewers.

#### References

- Andharia P.I.; Deheri, G. M.** (2010): Longitudinal Roughness Effect on Magnetic Fluid Based Squeeze Film between Conical Plates. To appear in *Industrial Lubrication and Tribology*, 62(5) .
- Andharia, P. I.; Gupta, J. L.; Deheri, G. M.** (1997): Effect of longitudinal surface roughness on hydrodynamic lubrication of slider bearings. *Proceedings of 10<sup>th</sup> International Conference on Surface Modification Technologies*, The Institute of Materials, pp. 872–880.
- Archibald, F. R.** (1956): Load capacity and time relations for squeeze films. *Trans. ASME*, vol. D78, pp. 231–245.
- Bhat, M. V.** (2003): *Lubrication with a magnetic fluid*, Team Spirit (India) Pvt. Ltd.
- Bhat, M. V.; Deheri, G. M.** (1991): Squeeze film behaviour in porous annular disks lubricated with magnetic fluid. *Wear*, vol. 151, pp. 123–128.

**Bhat, M. V.; Deheri, G. M.** (1992): Magnetic fluid based squeeze film between two curved circular plates. *Bulletin Cal. Math. Soc.*, vol. 85, pp. 521–524.

**Burton, R. A.** (1963): Effect of two dimensional sinusoidal roughness on the load support characteristics of a lubricant film. *J. Basic Eng., Trans. ASME*, vol. 85, pp. 258–264.

**Christensen, H.; Tonder, K. C.** (1969a): Tribology of rough surfaces: stochastic models of hydrodynamic lubrication. SINTEF Report No. 10/69 – 18.

**Christensen, H.; Tonder, K. C.** (1969b): Tribology of rough surfaces: parametric study and comparison of lubrication models. SINTEF Report No. 22/69 – 18.

**Christensen, H.; Tonder, K. C.** (1970): The hydrodynamic lubrication of rough bearing surfaces of finite width. Paper presented at the ASME – ASLE Lubrication Conference, Cincinnati, Ohio, paper 70 – Lub – 7.

**Deheri G.M.; Andharia P.I.; Patel R.M.** (2004): Longitudinally rough slider bearings with squeeze film formed by a magnetic fluid. *Industrial Lubrication and Tribology*, vol. 56, No. 3, pp. 177-187.

**Davies, M. G.** (1963): The generation of pressure between rough fluid lubricated, moving, deformable surfaces. *Lubr. Eng.*, vol. 19, p. 246.

**Guha, S. K.** (1993): Analysis of dynamic characteristics of hydrodynamic journal bearings with isotropic roughness effect. *Wear*, vol. 167, pp. 173–179.

**Gupta, J. L.; Deheri, G. M.** (1996): Effect of roughness on the behaviour of squeeze film in a spherical bearing. *Tribology Transactions*, vol. 39, pp. 99–102.

**Gupta, J. L.; Vora, K. C.** (1980): Analysis of squeeze films between curved annular plates. *Journal of Lubrication Technology*, vol. 102, pp. 48–53.

**Michell, A. G. M.** (1950): Lubrication, its principle and practice. p. 317 (Blackie, London).

**Murti, P. R. K.** (1975): Squeeze films in curved circular plates. *Journal of Lubrication Technology*, vol. 97, no. 4, pp. 650–654.

**Patel, R. M.; Deheri, G. M.** (2002a): Magnetic fluid based squeeze film between two curved plates lying along the surfaces determined by secant functions. *Indian J. Engg. and Mat. Sci.*, vol. 9, pp. 45–48.

**Patel, R. M.; Deheri, G. M.** (2002b): On the behaviour of squeeze film formed by magnetic fluid between curved annular plates. *Indian J. Math.*, vol. 44, no. 3, pp. 352–359.

**Patel, R. M.; Deheri, G. M.** (2007): Magnetic fluid based squeeze film between porous conical plates. *Journal of Industrial Lubrication and Tribology*, vol. 59, no. 3, pp. 143–147.

- Prajapati, B. L.** (1991): Behaviour of squeeze film between rotating porous circular plates: surface roughness and elastic deformation effects. *Pure and Appl. Math. Sci.*, vol. 33, nos. 1/2, pp. 27–36.
- Prajapati, B. L.** (1992): Squeeze film behaviour between rotating porous circular plates with a concentric circular pocket: Surface roughness and elastic deformation effects. *Wear*, vol. 152, pp. 301–307.
- Prakash, J.; Tiwari, K.** (1982): Lubrication of a porous bearing with surface corrugations. *Trans. ASME, J. Lub. Tech.*, vol. 104, pp. 127–134.
- Prakash, J.; Tiwari, K.** (1983): Roughness effects in porous circular squeeze – plates with arbitrary wall thickness. *J. Lub. Tech.*, vol. 105, pp. 90–95.
- Prakash, J.; Vij, S. K.** (1973): Load capacity and time height relations for squeeze film between porous plates. *Wear*, vol. 24, pp. 309–322.
- Ting, L. L.** (1975): Engagement behaviour of lubricated porous annular disks Part I: squeeze film phase, surface roughness and elastic deformation effects. *Wear*, vol. 34, pp. 159–182.
- Tonder, K. C.** (1972): Surface distributed waviness and roughness. First World Conference in Industrial Tribology, New Delhi, vol. A3, pp. 1–8.
- Tzeng, S. T.; Saibel, E.** (1967): Surface roughness effect on slider bearing lubrication. *Trans. ASME, J. Lub. Tech.*, vol. 10, pp. 334–338.
- Verma, P. D. S.** (1986): Magnetic fluid based squeeze film. *Int. J. Eng. Sci.*, vol. 24, no. 3, pp. 395–401.
- Wu, H.** (1970): Squeeze film behaviour for porous annular disks. *Transactions of ASME*, vol. F92, pp. 593–596.
- Wu, H.** (1972): An analysis of the squeeze film between porous rectangular plates. *Transactions of ASME*, vol. F94, pp. 64–68.